

# Mobile Physiological Measurement Platform With Cloud and Analysis Functions Implemented via IPSO

Wen-Tsai Sung, Jui-Ho Chen, and Kung-Wei Chang

**Abstract**—A physiological measurement platform is proposed for enabling users to measure physical condition regularly and to maintain good physical condition. The proposed system combines three basic physiological signal acquisition modules: an ECG module, a blood pressure module, and an oxygen saturation module. The physiological signals captured by the three physiological signal acquisition modules are sent via a data interface module to a mobile handheld device. Three communication systems are used for data transmission: RS-232 serial port wired transmission wireless, ZigBee, and Bluetooth. The captured physiological signals are presented on Android system mobile handheld devices, and the physiological data received by the mobile handheld device are sent to the cloud server via the Internet. After establishing a personal physiological database in the cloud server, the improved particle swarm optimization algorithm is used to determine the best personal physiological data, while setting physiological data dangerous levels for preliminary diagnosis. The dangerous levels are adjusted and set according to the personal medical records and physiological data of the subjects. When the physiological data reach the designated danger levels, it gives a warning to seek timely treatment by a medical unit. Finally, the system can incorporate video equipment to enable remote diagnosis and consultation by medical units.

**Index Terms**—Biomedical electronics, ZigBee, Bluetooth, Android, cloud.

## I. INTRODUCTION

ACCORDING to the 2011 statistics of the Council of Labor Affairs, fatigue caused 48 deaths in Taiwan. On average, one person died of fatigue, also known as Karoshi, every 7.6 days. Moreover, this statistical result is widely believed to have been deliberately manipulated by the government, and the actual number may be even larger. Overtime work is most common in the science and technology industry, the brokerage industry, the securities industry, and the health care industry. The term “Karoshi”, which means sudden death due to fatigue, was introduced by the Japanese medical personnel authority, TetsunojoUehata,

Manuscript received July 20, 2013; accepted August 26, 2013. Date of publication September 4, 2013; date of current version October 30, 2013. This work was supported by the National Science Council of Taiwan under Grant NSC 101-2622-E-167-006-CC3 and Grant NSC 100-2218-E-167-001. The associate editor coordinating the review of this paper and approving it for publication was Prof. Octavian Postolache.

The authors are with the Electrical Engineering Department, National Chin-Yi University of Technology, Taichung 41170, Taiwan (e-mail: songchen@ncut.edu.tw; chenjh@ncut.edu.tw; willy00325@gmail.com).

Color versions of one or more of the figures in this paper are available online at <http://ieeexplore.ieee.org>.

Digital Object Identifier 10.1109/JSEN.2013.2280398

TABLE I  
TEN LEADING CAUSES OF DEATH IN TAIWAN, 2011

Cause of death	Deaths	Death rate(100,000)	Percentage
All causes of death	152,030	655.5	100.00%
Malignancy	42,559	183.5	27.99%
Heart disease (except hypertension disease)	16,513	71.2	10.86%
Cerebrovascular diseases	10,823	46.7	7.12%
Diabetes	9,081	39.2	5.97%
Pneumonia	9,047	39.0	5.95%
Accidental injuries	6,726	29.0	4.42%
Chronic lower respiratory diseases	5,984	25.8	3.94%
Chronic liver disease and cirrhosis	5,153	22.2	3.39%
Hypertensive diseases	4,631	20.0	3.05%
Nephritis, nephrotic syndrome, and nephrosis	4,368	18.8	2.87%

who used the term to define continuous work harmful to psychological health. Disruption of the normal work and life pace of the worker leading to fatigue, long term overwork, worsening hypertension, and arteriosclerosis, can eventually result in death by exhaustion. Therefore, the proposed physiological integrated platform system was developed to provide a health management system for employees working in these fields to prevent them from dying of cardiovascular diseases [1].

According to a recent statistical analysis by the Taiwan Department of Health, the average life expectancy of males is 76.15 years while the average life expectancy of females is 82.66 years. This increased life expectancy indicates an aging population. Among the top ten causes of death in 2011 (Table 1), heart diseases ranked second, cerebrovascular diseases ranked third, and hypertensive diseases ranked ninth. Therefore, the seriousness of cardiovascular diseases cannot be ignored. Studies of the problems of reducing health care cost and improving health care efficiency show health care practices tend to spread from hospitals to patients, from the concentrated type to the dispersed type. Trends in the development of medical electronics include “miniaturization”, “portable”, “wireless”, “customization”, and “humanization.”

Disease management and health management plans should be “customized” to reduce medical costs [2].

This study of “medical electronics” combined two systems that have emerged in recent years: the “Internet of Things” (IOT) and “embedded Android software systems.” The IOT concept was proposed by Professor Ashton of MIT Auto-ID in 1999 in a study of RFID. The concept is that various objects can be connected by radio frequency identification message sensing equipment and the Internet to establish intelligent identification and management. In recent years, use of the IOT in daily life has grown rapidly in many areas, including transportation, environmental protection, public safety, home safety, industrial monitoring, elderly care, and personal health. The Android system, which is the mobile device operating system developed by the namesake company and by Andy Rubin, was purchased by Google in 2005. Several communication system manufacturers and hardware manufacturers later formed the “Open Hand-held Device Alliance” in 2007 to allow Android to become an official operating system of open original code. The system is now the most common operating system used in handheld devices (smart phone, Tablet PC) [3].

The above developments motivated this study to design a system platform for home measurement and remote monitoring. An integrated physiological measurement platform is used to collect simple measurements during daily life activity, e.g., blood pressure, hematocrit, and ECG, and a simple tablet PC is used as the display interface. When the system is used for measurement at home, the data are displayed on the Tablet PC in real time via the platform, which can be monitored remotely through the Internet. Finally, by adding cloud technology, the measured personal physiological data can be sent to the cloud system, via the Internet, to establish a personal health database [4].

## II. LITERATURE REVIEW

### A. Medical Electronics

No clear definition of medical electronics products has been established. In the past, medical electronics mainly referred to medical products that apply electronic technology; however, the increasingly complex and widespread application of technologies have gradually expanded the definition of medical electronics. Medical electronic products can be categorized in terms of functionality into three major categories: diagnostic equipment, medical treatment equipment, and rehabilitation equipment; subcategories of diagnostic equipment include physiological monitoring equipment, inspection equipment, and medical image products. Subcategories of medical treatment equipment include radioactive treatment equipment, dialysis and infusion equipment, respiratory and anesthesia equipment, powered surgical equipment, and hospital supplies. Subcategories of rehabilitation equipment include electronic aids and physical therapy equipment. The focus of this study is diagnostic equipment [5].

The sensing module of the proposed physiological measurement platform mainly consists of the multi-functional physiological sensing module established in references [6] and [7]. The main characteristics are (1) a low-power portable ECG signal inspection system; (2) capability to measure

blood pressure rapidly; and (3) capability to measure oxygen saturation. A set of medical instruments satisfying the above conditions are developed. The advantages include low cost and portability. The major sensing modules for measuring ECG, blood pressure, and oxygen saturation were applied as mentioned in the references. However, this study differs from earlier studies in that the displayed data are sent to a mobile phone *via* Bluetooth for calculation and display of the patient’s status [8].

### B. Medical IOT

The concept of the IOT was proposed by Kavin Ashton of MIT in 1999. It mainly connects all objects by radio frequency identification message sensing equipment to provide intelligent identification and management. The IOT integrates information sensing devices, e.g., radio frequency identification system (RFID), infrared sensor, global positioning system, and laser scanners to connect with the Internet. The IOT can be divided into three components: (1) sensing end: performs object identification or sensing, e.g., sensors or radio frequency identification tags; (2) network transport layer: transmits data to the end platform via the Internet; and (3) application and service end: processes the information according to data attributes and shares and provides subsequent service applications. The IOT has very many applications. For example, objects to be identified and managed can be incorporated in many IOT applications, including transportation, environmental protection, governmental work, public safety, home safety, firefighting, industrial monitoring, elderly care, personal health, etc. This study applied the concept of IOT to personal health management. As mentioned in [9], medical IOT can be subdivided into three aspects: (1) thing-object, for example: doctor, patient, medical equipment, etc.; (2) connection—information exchange, for example: medical records; and (3) network—the process of information exchange; applying IOT technology can enhance many aspects of hospital management, including medical equipment management, medical pharmaceuticals management, personal medical records management, medical personnel, and patients [10].

### C. Mobile Handheld Device-Android System

The Android system is an open hand-held equipment platform operating system based on the Linux kernel. Android was originally the operating system for mobile devices such as mobile phones but has gradually been extended to tablet PCs and other devices such as E-book readers, MP4 players, Internet TVs, etc. Android currently has the largest share of the mobile handheld device market. The Android system architecture can be mainly divided into the five parts shown in Fig. 1 [11], [12].

- 1) Bottom layer-Linux kernel: this kernel controls hardware drivers, power supply, network, system security, and memory management.
- 2) System layer-libraries: these libraries contain numerous open source codes, including: C language libraries Libc, SQ Lite, OpenSSL, libraries for webpage browsing, and various multi-media libraries in support of players.

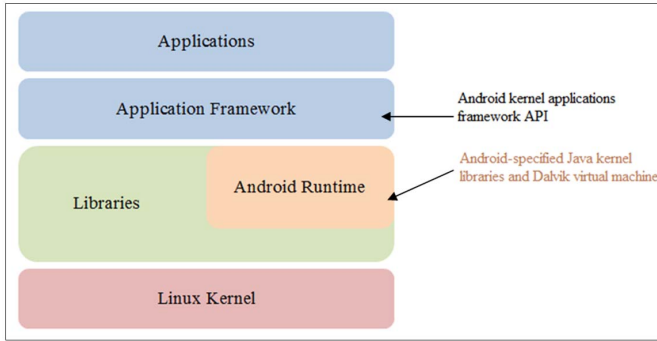


Fig. 1. Android system architecture diagram.

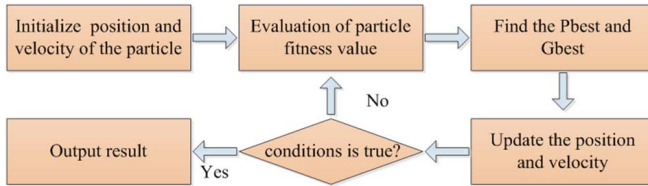


Fig. 2. Particle swarm optimization flowchart.

- 3) Android runtime: this group of Android-specified Java kernel libraries and Dalvik virtual machine convert Java executable code Bytecode into the Android Dalvik Executable (.dex) so that users can write Android applications and run multiple applications.
- 4) Application framework (API): this set of Android kernel applications framework APIs allows convenient use of common application design architectures by program developers and increases application development velocity.
- 5) Application layer: Java language kernel applications, including mailbox, message, calendar, browser, and other common applications for the convenience of users.

#### D. Particle Swarm Optimization

Particle swarm optimization (PSO) was first proposed by Kennedy and Eberhart in 1995. Initially, this method was used to search for the maximum benefits of a group by observing the movements of flocks of birds and schools of fish. For example, PSO can simulate the hunting behaviors of a flock of birds. A flock of birds randomly searches for food in an area when food is present. However, not all the birds know where the food is or how far it is from the present location. Therefore, the problem is determining the optimal strategy for finding food. The simplest and most effective way is to search the area surrounding the bird closest to the food [13], [14]. Figure 2 shows the steps of PSO:

Step 1. Initialize the population, and determine the initial position and velocity of each particle in a random manner. These random particles should be limited in the specified range;

Step 2. Input the particle position into the solution problem evaluation function to calculate the value of each particle;

Step 3. Compare the evaluation value of each particle and the optimal evaluation value of the particle. If the new

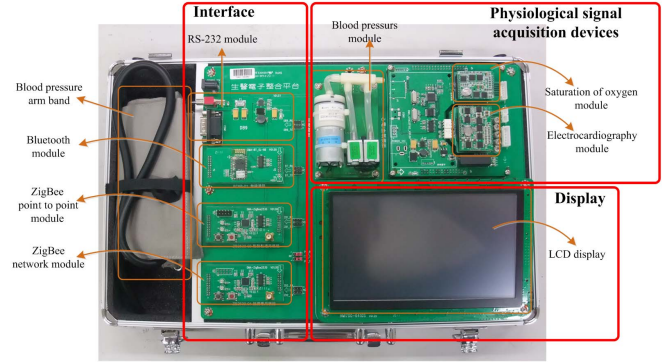


Fig. 3. Image of implemented physiological measurement platform.

evaluation value is better than the optimal evaluation of the particle, replace the optimal solution location and evaluation value with the new optimal solution location and evaluation value, respectively;

Step 4. Compare the optimal evaluation value of each particle and the optimal evaluation value of all particles, and if the optimal evaluation value of the particle is better than optimal evaluation value of the group, use the optimal solution position and evaluation value of the particle to replace those of all other particles;

Step 5. Change particle velocity and position according to Eqs. (2) and (3);

Step 6. Determine whether the ending conditions have been satisfied; if not, return to Step 2; otherwise, output the results.

### III. HARDWARE ARCHITECTURE AND SYSTEM COMPOSITION

Figure 3 shows the four categories of major devices: physiological signal acquisition devices, transmission devices, rear end display devices, and cloud server; Fig. 3 shows the three physiological signal acquisition modules: an electrocardiography module, a blood pressure module, and an oxygen saturation module. The acquired physiological data are transmitted via the interface module (RS-232, ZigBee, and Bluetooth) to the rear end display devices (mobile handheld device). Finally, the physiological data are uploaded to the system rear end cloud server through the network, and IPSO is used to determine the optimum values of the physiological data so that the danger level can be set. When the danger level is set, the physiological data can be used for preliminary analysis and diagnosis. Figure 4 is a diagram of the system architecture, which resembles those presented in [15] and [16].

#### A. Electrocardiography Module

The ECG signal is one of many physiological signals of the human body. The ECG signal behavior originates from the SA node, also called a cardiac pacemaker, which is a group of specialized neural intramuscular fibrous tissue on the right atrial wall. On average, depolarization occurs 60-100 times per minute. When depolarization of the SA node begins, the electrical pulse is used to contract the left and right atriums.

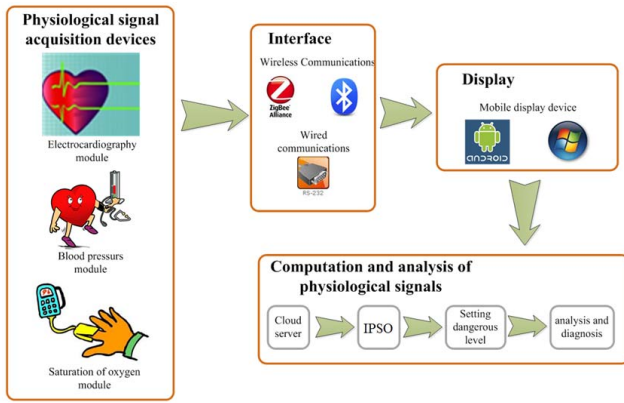


Fig. 4. System architecture diagram.

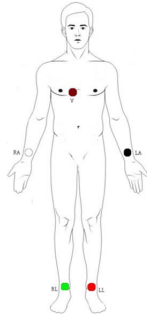


Fig. 5. Six-lead electrode patch location.

The pulse is then sent to the AV node between the left and right ventricles. Transmission of the pulse between the left and right bundle branches causes the left and right ventricles to contract and transfer blood throughout the body; therefore, the gap between contraction of the atrium and ventricle is between 0.12 to 0.20 seconds [17].

The signal range was set to 0.5 HZ~125 HZ. Figure 5 shows that the sampling lead procedure used in the Six-lead system was I, II, III, aVR, aVL, and aVF; this module uses a serially connected port to provide the highly accurate and reliable dual direction communication and computation needed for fast and accurate ECG measurements. The advantages of this module are its small volume and low power consumption [18]. The module principle is as shown in Fig. 6 while Fig. 7 illustrates the ECG experimental procedure diagram.

### B. Blood Pressure Module

The WHO/ISH Guideline Committee and Joint National Committee (JNC) defines hypertension as blood pressure above 140/90 mmHg and defines normal blood pressure as blood pressure lower than 130/85 mmHg. Blood pressure measurement can generally be classified as invasive or non-invasive [19].

The non-invasive blood pressure measurements performed in this study included the oscilloscope amplitude method and the listening diagnostics method. The oscilloscope amplitude method is performed as follows. During the compression and decompression process, an occluding cuff is used to measure the effect of vibration caused by the heartbeat on the blood

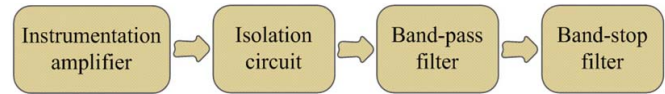


Fig. 6. ECG module schematic diagram.

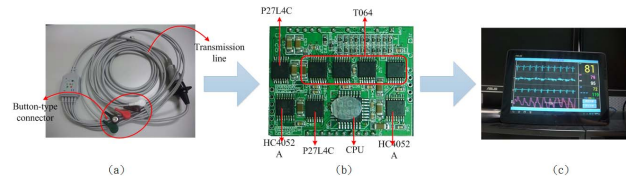


Fig. 7. (a) ECG leads retrieve line, (b) ECG module, (c) Display interface.

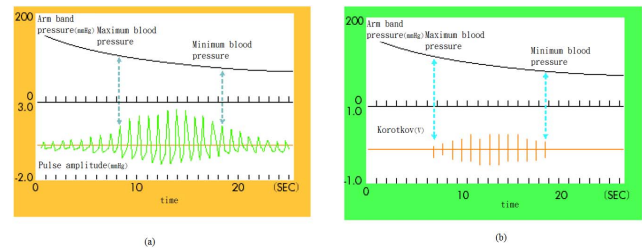


Fig. 8. (a) Oscillometry schematic diagram. (b) Ripa Rocci Korotkov schematic diagram.

vessel wall in terms of changes in the pressure of the occluding cuff (pulse pressure), which are used to test the pressure amplitude of the occluding cuff and determine the blood pressure value. Figure 8(a) shows that, generally, when the pulse pressure dramatically increases, the occluding cuff pressure is the “highest blood pressure”; when the occluding cuff pressure dramatically decreases; the occluding cuff pressure is the “lowest blood pressure”.

The listening diagnostics method, also known as the auscultation method, was proposed by the Russian physician Korotkoff in 1905. When the occluding cuff pressure decreases, the blocked blood flow works with the pulse of the heart. Figure 8(b) shows that the sound of the blood vessel when the blood starts to flow slowly is known as the Korotkov sound = K sound, the occluding cuff pressure when the K sound is detected is the “highest blood pressure”, and the occluding cuff pressure when the K sound disappears is the “lowest blood pressure”. This study used the oscilloscope amplitude method to measure blood pressure, which is the most common method. The module proposed in this study uses dual direction serially connected port communication and computation to enable accurate, reliable, and rapid blood pressure measurements. The principles of the blood pressure module are shown in Fig. 9 while Fig. 10 illustrates the blood pressure measurement experimental procedure [20].

### C. Oxygen Saturation Module

In human blood, 45% of the cells are red blood cells, including 30% hemoglobin (Hb). The main function of hemoglobin is to transport oxygen and carbon dioxide to human tissues. The combination of hemoglobin and oxygen is known as the oxygenated hemoglobin ( $O_2Hb$ ), which

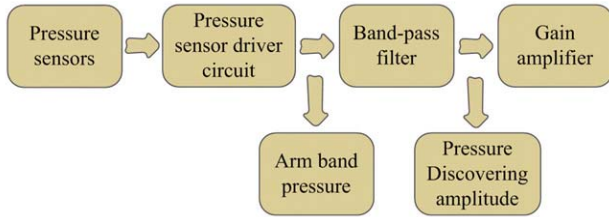


Fig. 9. Blood pressure module schematic diagram.

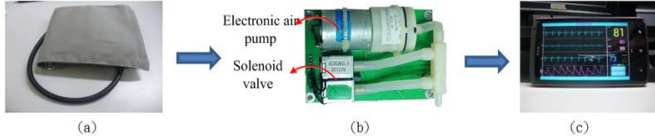


Fig. 10. (a) Blood pressure arm band, (b) Blood pressure module, (c) Display interface.

takes oxygen to organs and tissues. Oxygen transported to tissues leaves hemoglobin, which is then called the reduced hemoglobin ( $Hb$ ). Next, hemoglobin takes up carbon dioxide and becomes carbon dioxide hemoglobin. Oxygen saturation refers to hemoglobin in blood ( $SaO_2$ ), and is defined as shown in Eq. (1) [21]

$$SaO_2 = \frac{O_2Hb}{O_2Hb + Hb} \times 100\%. \quad (1)$$

In this study, the probe of the pulse oxygen saturation instrument is similar to that shown in the diagram. The probe can be used in areas such as the fingertip, finger, or earlobe, where the tissue layer is thinner and filled with micro blood vessels and circulating blood. These areas are also very suitable measurement points for oxygen saturation measurement. Two LED (Light Emitting Diode) light sources of different wavelengths are fixed; the light emitting wavelengths are 660 nm red light and 940 nm infrared light, respectively. A photoelectric sensor at the lower end converts the red light and the infrared light into electric signals (A/D converter). As the optical signals absorbed by the tissues, bones, and blood increase, the detected signal decreases. The proposed module uses a dual-wavelength photoelectric testing platform and can exchange of various wavelengths by performing extension protocols. The DC signal waves can be provided for other applications; pulse blood oxygen measurement is a typical application. The principles of the oxygen saturation modules are as shown in Fig. 11. Figure 12 is a diagram illustrating the oxygen saturation and concentration experimental procedure.

#### D. ZigBee Module

ZigBee is another term for the IEEE 802.15.4 protocol for short-distance, low-power, wireless communications. ZigBee is characterized by a short range, low complexity, low power consumption, low data transfer rate, and low cost. The protocol is mainly used in home device automation, environmental security and control, personal medical care, automatic control and remote control, and various embedded equipment [22].

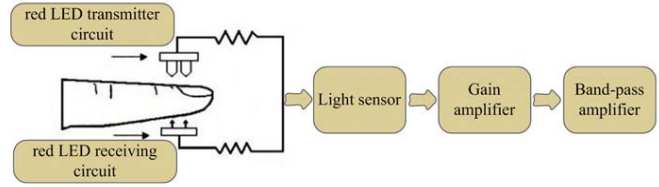


Fig. 11. Oxygen saturation schematic diagram.

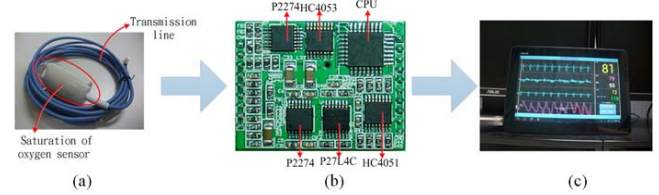


Fig. 12. (a) Oxygen saturation sensor, (b) Oxygen saturation module, (c) Display interface Medical electronics.

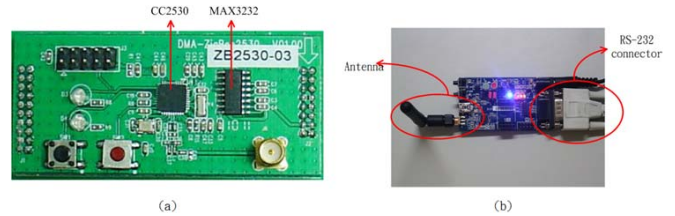


Fig. 13. (a) ZigBee sender module, (b) ZigBee receiver module.

In this study, ZigBee was used to establish a self-organizing network to transfer biomedical module data to the end equipment. The network function was then used to display the data on various remote display equipment. Figure 13 shows the sender module at one end and the receiving module at the other end. The receiving module connects to the computer via RS-232 to display the processed data [23].

#### E. Bluetooth Module

Bluetooth was introduced in May 20, 1999. Industrial leaders, including Sony Ericsson, IBM, Intel, Nokia, and Toshiba, founded the “Special Interest Group” (SIG), which is the predecessor of the Bluetooth alliance. The purpose of the SIG was to develop a set of Bluetooth technology standards to enable low-cost, highly-efficient, short-distance random wireless connections. Bluetooth which is the open standard for wireless data and voice transmission is used for wireless connections of various communication equipment, computer and end equipment, various digital data systems, and even household electric appliances. Its transmission distance is typically 10 cm ~ 10 m but can be increased to 100 m by adding peripherals. In this study, Bluetooth technology is used to transmit data to the display interface and to enable remote monitoring. Figure 14 illustrates the Bluetooth module and Bluetooth receiving module. For PCs that do not have Bluetooth capability, a connection can be realized by installing a receiver module [24].

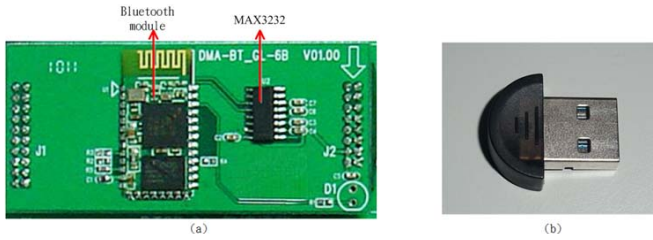


Fig. 14. (a) Bluetooth module, (b) Bluetooth receiver module.

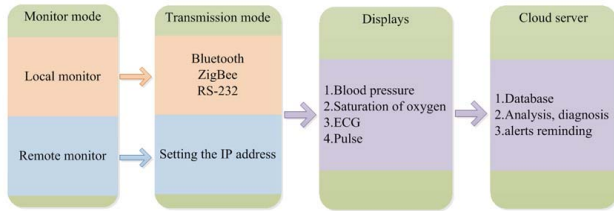


Fig. 15. Software architecture flowchart.

#### IV. SOFTWARE ARCHITECTURE

Measurement data were displayed on mobile hand-held equipment to enable local and remote monitoring. For local monitoring, the mobile hand-held equipment is directly connected to the frontend physiological signal acquisition platform to enable immediate display of physiological data on the mobile hand-held equipment. Remote monitoring requires the installation of a fixed network address at the local end. The network address connection enables mobile hand-held equipment to access the physiological data for the subject. Finally, the data are uploaded to the cloud server, a personal database is established for the subject at the server end, and the diagnostic conditions for various diseases are set for the preliminary diagnosis (See Fig. 15) [25].

#### V. IMPROVED PARTICLE SWARM OPTIMIZATION (IPSO) ALGORITHM MODEL

The objective of this study was to apply the system identification method can be decomposed into sub-models choice (that is, the system structure identification) problems and model parameters identification problem. To choose the best-fitting sub-model from sub-models belonging to a class of combinatorial was optimization problems [26].

When selecting a set of mathematical models with an unknown structure, no standard method of identifying the parameters has been developed, and the parameter identification problem is a class of optimization problems. The PSO algorithm is a global random optimization algorithm that has been successfully used in many fields and is widely considered effective for solving combinatorial optimization problems and parameter optimization problems because of its effectiveness for system identification [27].

Particle Swarm Optimization algorithm is a community-based evolutionary algorithm. Each of the first random initialization particles in the solution space has its own position

and speed, as well as a decision by the optimization function adaptation value. The particle tracks two “extreme” values and updates them iteratively. The first extreme value of the particle itself can find the optimal solution, which is called the individual extreme point (Pbest); the other extreme is the optimal solution found by the particle populations, which is called the global extreme point (Gbest). Suppose, in a D-dimensional space, particle information is available to indicate a D-dimensional vector. The  $i$ -th position of the particle can be expressed as  $X_i = (x_{i1}, x_{i2}, \dots, x_{iD})$ , velocity can be expressed as  $V_i = (v_{i1}, v_{i2}, \dots, v_{iD})$ , the particle search to Pbest is  $P_i = (p_{i1}, p_{i2}, \dots, p_{iD})$ , Entire particle swarm search to G best is  $P_g = (p_{g1}, p_{g2}, \dots, p_{gD})$ . After the two optimal solutions are found, the particle speed and position are updated according to (2) and (3), respectively.

$$v_{id}(t+1) = v_{id}(t) + c_1 r_1 (p_{id} - x_{id}(t)) + c_2 r_2 (p_{gd} - x_{id}(t)) \quad (2)$$

$$x_{id}(t+1) = x_{id}(t) + v_{id}(t+1) \quad (3)$$

$V_{id}$	velocity of each particle in d dimension;
$w$	inertia weight;
$c_1, c_2$	learning constant;
$rand()$	random number between 0 and 1;
$P_{id}$	the optimal position of each particle up to the present;
$P_{gd}$	the optimal position of all particles/group up to the present;
$X_{id}$	the position of each particle up to the present.

In the above equations:  $i = 1, 2, \dots, N$ ;  $d = 1, 2, \dots, D$ ;  $c_1$  and  $c_2$  are non-negative constant;  $r_1$  and  $r_2$  is a uniformly distributed random number between  $[0, 1]$ ;  $v_{id} \in [-v_{max}, v_{max}]$ ,  $v_{max}$  is maximum rate by set before;  $t$  is the current number of iterations. The purpose of system identification is to ensure that the system output  $y(t)$  is as close as possible to the known system output  $y_0(t)$ . Very similar values indicate a good fit to the description. The following criterion is used for the fitness function

$$f = \sum_t [y(t) - y_0(t)]^2. \quad (4)$$

Practical applications of the BPSO algorithm have shown several limitations. The main limitation is that the BPSO is prone to premature convergence and has poor local optimization. Thus, some researchers have attempted a series of improvements to the BPSO algorithm. Our previous works, *i.e.*, [28]–[31], introduce the inertia weight  $\omega$  for Eq. (4) velocity items,

$$v_{id}(t+1) = \omega v_{id}(t) + c_1 r_1 (p_{id} - x_{id}(t)) + c_2 r_2 (p_{gd} - x_{id}(t)) \quad (5)$$

This study also proposes an inertia factor decreasing strategy, *i.e.*,

$$\omega = -(\omega_{start} - \omega_{end}) \left( \frac{t}{t_{max}} \right)^2 + \omega_{start} \quad (6)$$

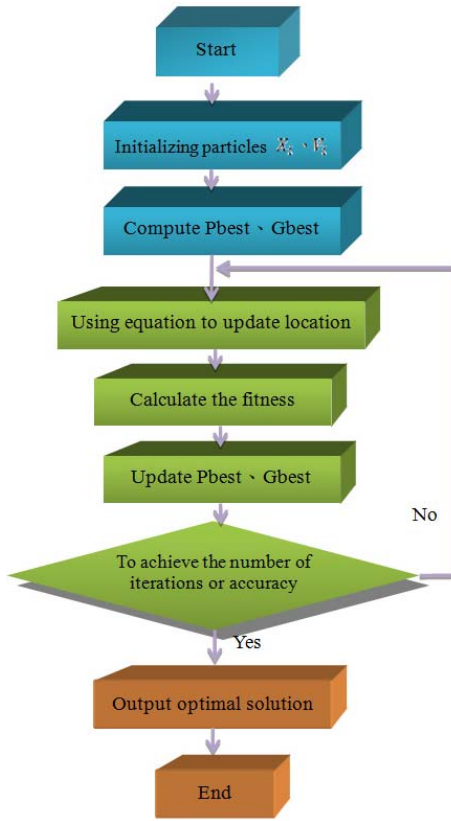


Fig. 16. IPSO algorithm model flowchart.

In Eq. (6),  $t_{max}$  is the maximum number of iterations;  $\omega_{start}$  and  $\omega_{end}$  are inertia factors for the initial and maximum number of iterations. This study also proposes each velocity update. In addition to the exchange itself Reflection and with the addition of a particle, the particle is also considered the average value for the entire population.

$$v_{id}(t+1) = \omega v_{id}(t) + c_1 r_1 (p_{id} - x_{id}(t)) + c_2 r_2 (p_{gd} - x_{id}(t)) + c_3 r_3 (p_{ad} - x_{id}(t)) \quad (7)$$

In Eq. (7),  $P_a = (p_{a1}, p_{a2}, \dots, p_{aD})$  is the  $t$ -th generation and the Pbest average of all particles.  $p_{ad}$  is the  $d$ -th component of the  $P_a$ ;  $c_3$  is non-negative constant;  $r_3$  is a uniformly distributed random number.

This study integrated Eqs. (5–7) and proposed the improved particle swarm optimization (IPSO) algorithm model shown in Fig. 16.

Out of all adjustable parameters of the IPSO algorithm, inertia weight is the most important improvement parameter because it determines the effect of the previous flight speed of the particle on the current flight speed of the particle. Therefore, the inertia weight value can be adjusted by balancing the global and local search. This study experimentally changed value  $w$  in Eq. 6. In the early stage of evolution in the IPSO algorithm,  $w$  slowly decreases. Therefore, the global search capability of the system is very strong, which is helpful for finding good optimization seeds. In the late stage of the evolutionary algorithm, the decreasing trend in  $w$  accelerates. Therefore, a suitable seed must be found early

to increase the convergence speed of the algorithm. This calculation process avoids the limitations of the typical linear decreasing strategy and greatly improved the IPSO algorithm performance.

## VI. EXPERIMENTAL IMPLEMENTATION AND ANALYSIS

This study used the integrated physiological measurement platform to measure ECG, blood pressure, and oxygen saturation. For ECG measurement, electrode patches were attached to the subject, and the captured signals were filtered and displayed by the signal capture module. When measuring blood pressure, the subject must wear a pressure arm band. Two pressure values obtained by the blood pressure sensing module are used to calculate the blood pressure value. The measurement of oxygen saturation requires the subject to wear the oxygen saturation sensing device on a finger. The oxygen saturation sensing device is installed with two LED lights of different wavelengths. The Lambert-Beer law of light absorption is then applied to test the oxygen concentration in the blood, and the blood oxygen module can be used to calculate the measurement data to obtain an accurate oxygen saturation value. Finally, all results can be displayed on a mobile hand-held device [32] such as a Tablet PC or mobile phone.

The diagram below shows that physiological data captured by sensing devices worn by the user are displayed on a computer or on a mobile device such as a Tablet PC or smart phone [33] before being uploaded to the cloud server. Moreover, Fig. 17 shows that doctors in the medical unit can use the video equipment to diagnose the subject or to engage in dialogue.

After the signal captured by the physiological signal acquisition module has been sent to the portable mobile device (*e.g.*, smart phones, tablet PCs) or to the user PC, physiological data such as ECG, blood oxygen, and blood pressure are sent to the A/D converters. A serial port is then used to send and display the analysis and diagnosis to portable mobile devices through Bluetooth or to a PC through ZigBee. If the physiological signals of the user are abnormal, an SMS is sent to the care giver of the patient, and the data are sent to the cloud server. The physicians can review the data stored on the computer, and, if necessary, advise the patient by using video chat (Refer to Figs. 18 and 19).

Figures 20(a–d) compare the proposed integrated platform equipment and general commercial equipment in terms of blood pressure and oxygen saturation measurement. The horizontal axes in Figs. 20(a–d) represent the measurement data quantity while the vertical axes represent the measurement data type. The diagrams confirm that the equipment used in this study is highly accurate.

A commercially available standard sphygmomanometer (OSTAR, Biomedical Technology Corp) was used as a basis of comparison. It has developed the world's patents spectrum of cardiac monitoring technology. The system includes a blood pressure meter that can be used for general inspection and a digital signal processor that calculates heart noise for medical reference.

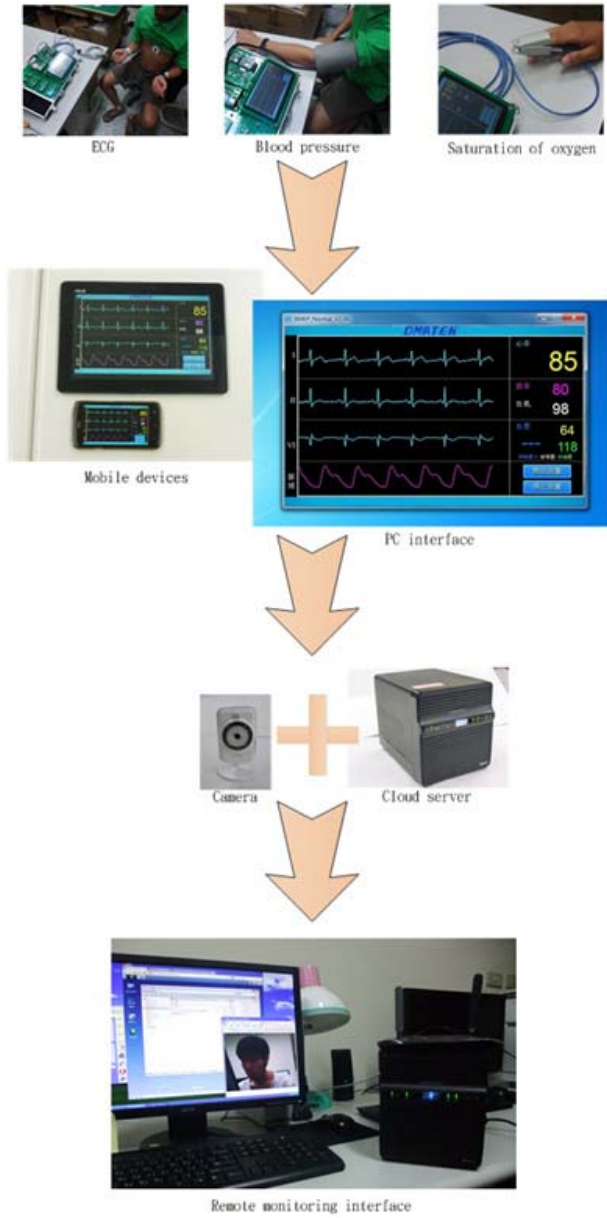


Fig. 17. Actual measurement flowchart system.



Fig. 18. Actual measurement display interface.

Equations 8–9 show the calculation for changes in blood pressure with age:

$$\text{Systolic Blood Pressure (SBP)} = (104 + (\text{years} \times 0.3)) \times 1\text{mmHg} \quad (8)$$

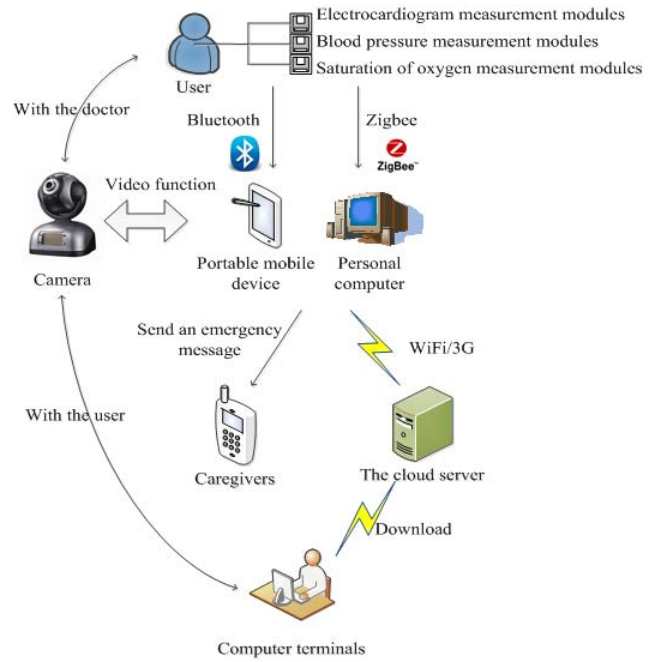


Fig. 19. System architecture schematic diagram.

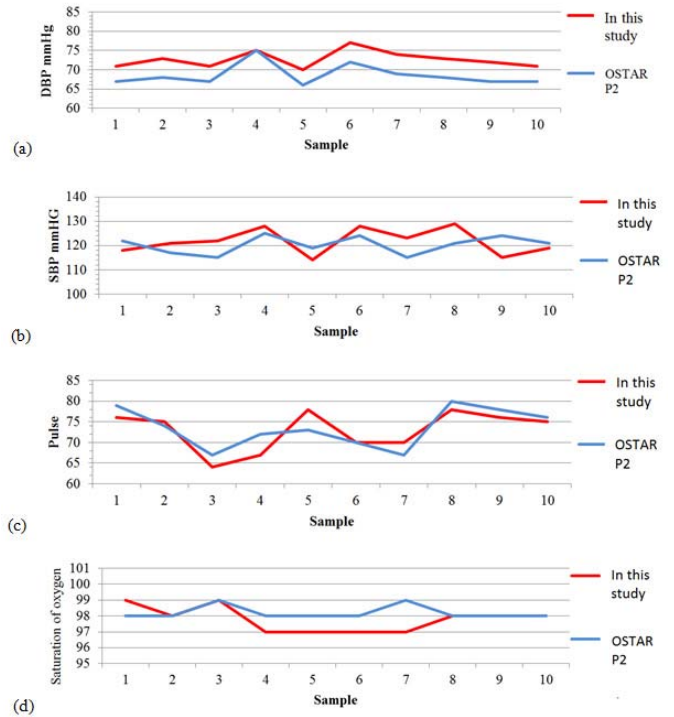


Fig. 20. (a) DBP comparison. (b) SBP comparison. (c) Pulse comparison. (d) Oxygen saturation comparison.

Diastolic Blood Pressure (DBP)

$$= (70 + (\text{years} \times 0.3)) \times 1\text{mmHg} \quad (9)$$

Mean Blood Pressure (MAP)

$$= \frac{1}{3}\text{SBP} + \frac{2}{3}\text{DBP}. \quad (10)$$

To find the optimal physiological data for the subject, these equations can be used before applying IPSO. Optimal physiological data were calculated for all ages starting



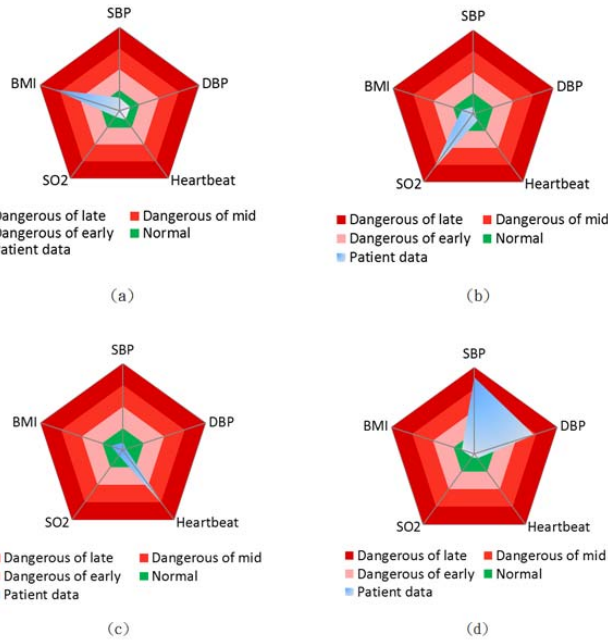


Fig. 21. Physiological data index chart. (a) BMI value indicating patient is overweight, (b) oxygen saturation is deficient, (c) heartbeat is too fast, (d) blood pressure is too high.

at age 11 years and then at five year intervals. For example, for people aged 21 ~ 25, the optimal values are systolic pressure at 111.5 mmHg, diastolic blood pressure at 78 mmHg, heartbeat at 72, and oxygen saturation at 98%. These values are used as judgment standards. Figure 21 shows how the various physiological data are depicted in a radar chart in order to determine the danger level of the physiological conditions. Regarding subjects suffering from specific diseases, the proposed method can set different diagnosis conditions. For example, subjects with hypertension stress and hypertension acute diseases are reminded about drug use. Equation (10) can then be used test whether the condition of the subject has become normal. If the standards are not satisfied, a warning is given. Within 24 hours after taking medication, patients with hypertension stress can reduce their mean artery blood pressure by up to 25%; patients with hypertension acute diseases can reduce their mean artery blood pressure by up 10% within one hour after medication and by 15% within two hours after medication [34], [35].

Finally, weights are set according to the danger level. For physiological data in the normal range, the weight is set to 0.5. For physiological data above the normal range, the weights are set according to severity; for example: if the oxygen saturation is 94% ~ 92%, the weight is set to 3. Since the literature indicates that oxygen saturation is an important element in the human body, its weight is set higher than that of other physiological indicators. Tables 2–4 show how the weight and measurement values are set for each interval. Table 5 shows that a normal subject has a total weight of 3. If the total weight equals or exceeds 6, it sends a help message; if it equals or exceeds 8, it sends an emergency warning; if it equals or exceeds 10, it sends a warning of loss of consciousness.

TABLE II  
BLOOD PRESSURE CLASSIFICATION

Classification	SBP	DBP	Weight value
Hypotension	<90	<50	2
Normotensive	90~120	50~80	1
Hypertension of early	120~139	80~89	2
Hypertension of mid	140~159	90~99	3
Hypertension of late	$\geq 160$	$\geq 100$	4

TABLE III  
CLASSIFICATION OF OXYGEN SATURATION

Dangerous level	One	Two	Three	Normal
	First aid	Critical	Urgent	Normal
Saturation of Oxygen ( $SO_2$ )	<90%	90%~92%	92%~94%	>95%
Weight value	8	6	4	1

TABLE IV  
CLASSIFICATION OF PULSE

Heart rate	<64	65~80	80~95	>96
Judgment result	Slow	Normal	Fast	Too fast
Weight value	2	1	3	4

TABLE V  
CLASSIFICATION OF WEIGHT VALUE

Weight value	Dangerous level
3	Normal
3~6	Dangerous of early
6~8	Dangerous
8~10	Dangerous of mid
10~	Dangerous of late

## VII. EXPERIMENTAL RESULTS DISCUSSION

### A. Improve PSO Results

This study illustrates the potential performance gains obtained by the derived optimal multi-sensor precise measurement by applying the data fusion allocation scheme. The fading coefficients of the channel between the sensors and the fusion center are assumed to be the total length of the particle  $n_1 + n_2 + \dots + n_{5-1} + 1$  distributed with a unit mean.

In the experimental analysis of the proposed system, this study set,  $n_s$ , *i.e.*, the number of multiple wireless sensors, to 20, 50, 120, and 180. Table 6 shows that, when the number of sensor signals is large, the proposed IPSO algorithm obtains more accurate measurement results compared to normal mode and compared to conventional PSO. This observation is most apparent when  $n_s > 110$  (Refer to Fig. 22).

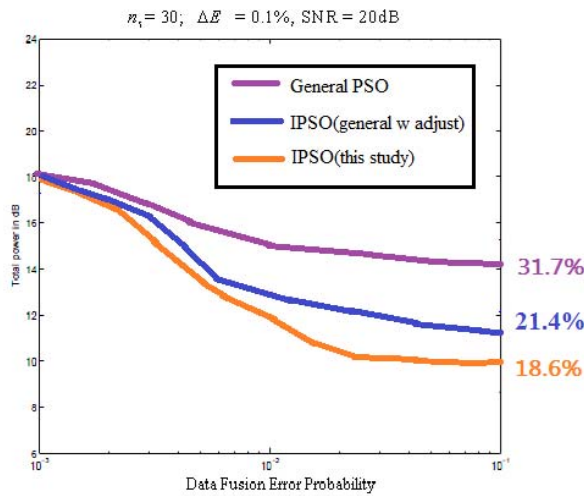
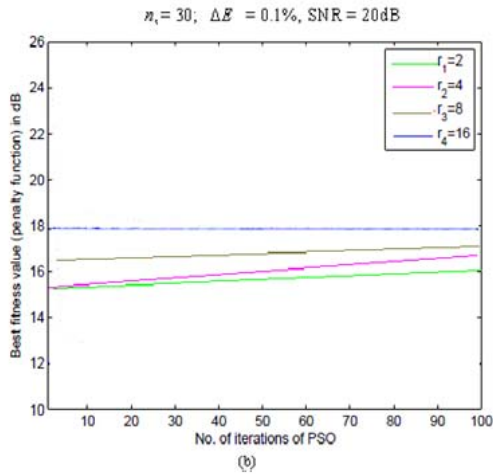
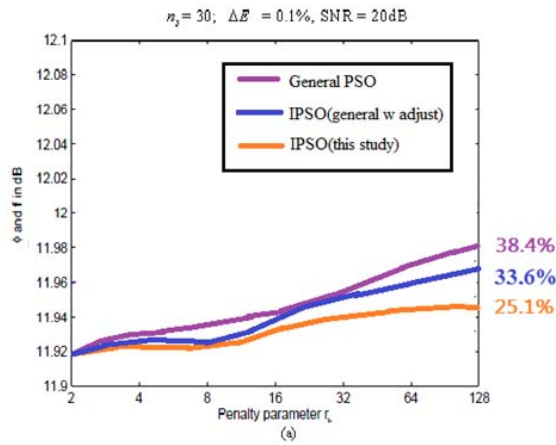


Fig. 22. Convergence of exterior penalty function-based IPSO: multi-sensor data fusion error probability is below 0.01%. (a) Best fitness returned for IPSO iterations for a given penalty parameter. (b) Convergence of penalty function to the original optimization problem. (c) IPSO data fusion error probability when observations are correlated ( $n_s = 30$ ;  $\Delta E = 0.1\%$ ,  $\text{SNR} = 20$  dB).

### B. Comparison of Blood Pressure Measuring Instruments by Proposed Measurement With Commercially Available Blood Pressure Instrument

To compare error values in research equipment and instruments currently in use, subjects used two instruments

TABLE VI  
COMPARATIVE ANALYSIS OF CALCULATED IN IMPROVE PSO  
EXPERIMENTAL ( $n_s = 20, 50, 120, 180$ )

$n_s$	Approaches	Average error rate%	Convergence %	Iterations%	Success %
20	Non-PSO	<0.001	94.1	47.1	92.1
	PSO	<0.001	96.3	48.9	91.8
	IPSO(general)	<0.001	97.4	52.7	92.0
	IPSO(this study)	<0.001	97.2	50.2	92.3
50	Non-PSO	<0.24	87.8	63.8	83.2
	PSO	<0.16	89.3	58.2	86.6
	IPSO(general)	<0.051	94.1	56.5	88.9
	IPSO(this study)	<0.071	95.5	52.3	91.2
120	Non-PSO	<0.53	81.3	68.2	80.1
	PSO	<0.51	83.5	70.3	83.2
	IPSO(general)	<0.35	91.4	66.3	86.3
	IPSO(this study)	<0.28	93.9	62.8	92.8
180	Non-PSO	<0.95	64.2	75.2	85.1
	PSO	<0.73	72.8	68.2	88.2
	IPSO(general)	<0.41	83.9	67.5	89.7
	IPSO(this study)	<0.22	88.1	63.1	93.7

simultaneously to obtain fifty measurements. Figures 23–24 compare the proposed system and existing systems in real time in terms of average distortion and average sensitivity. Existing wireless remote care systems developed by Frontline Test Equipment Inc. (Charlottesville, VA, USA) and Ke Chuang Technology Inc. (Shenzhen, China) were used in the two experiments. The first experiment observed the instrument measurement in error ratio value. The second experiment obtained 20 wireless measurements of Multi-Physiology Signals Fusion and computed the error ratios.

Figure 23 shows the instrument measurement results. The horizontal axis represents the measured data, and the vertical axis represents the numerical results for blood pressure. The statistical results indicate that use of the present system in a commercially available blood pressure instrument obtains an error rate of 5%.

Since the focus of this study was the use of wireless devices for transmitting physiological information, further experiments were performed using a platform of wireless transmission equipment built using commercially available equipment (wireless transmission parts). The experiment measured three items: blood pressure, heart rate and blood oxygen concentration.

Figure 24 compares the error results obtained after 50 measurements. The horizontal axis represents the measured data, and the vertical axis represents the numerical results of blood pressure. The statistical results revealed a blood pressure equipment error approximating 6% and a heart rate and blood oxygen concentration equipment error approximating 6%. For the devices used in this study, the accuracy of physiological signal error converged within the range of 10%, which indicated that accuracy was higher than that in the conventional wireless physiological signal measurement platform.

### C. IPSO Weight Simulation Results

In this study, the physiological system is applied to enter private groups and staff regular physiological numerical measurement. Since the effects of a disease may accumulate slowly over time, long-term data must be included in the data library.

Since the database containing long-term cumulative data is very large, searches of data for sick staff are very time

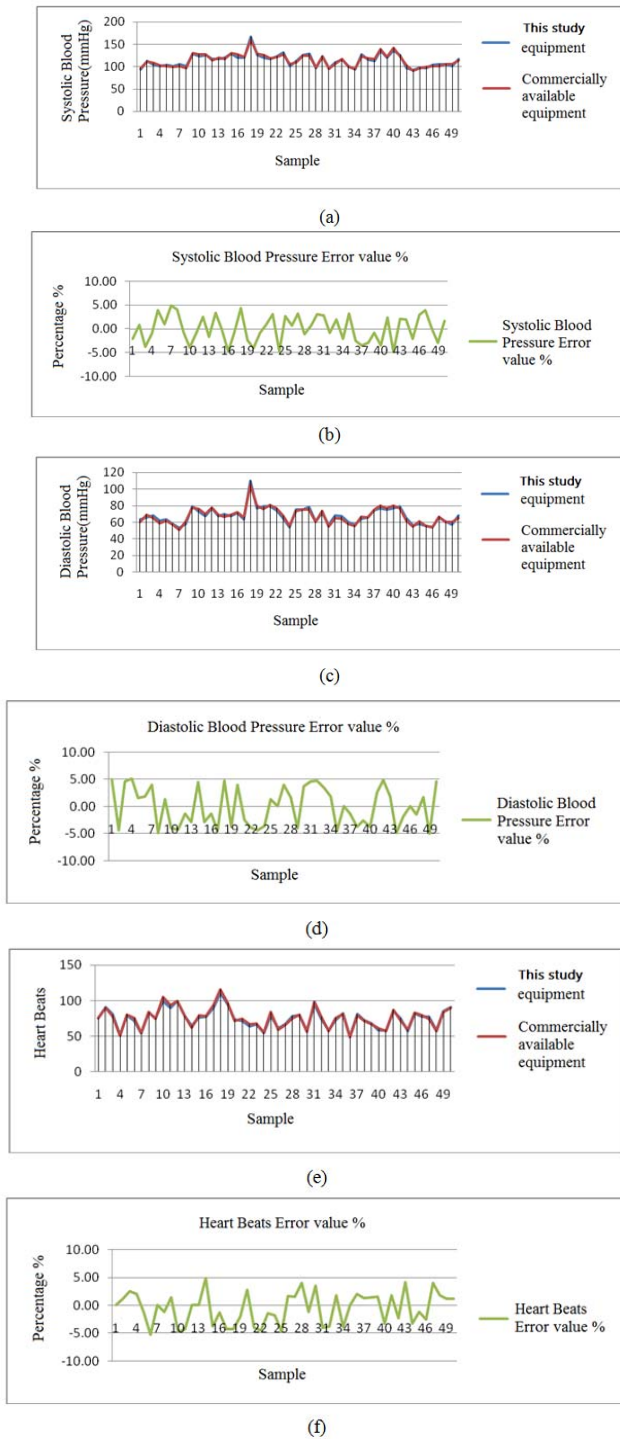


Fig. 23. Comparison of measurements in this study with existing instrument measurement in terms of error ratio value. (Wired transmission environment-based) (a) Systolic blood pressure measurements. (b) Systolic blood pressure measurement error curve. (c) Diastolic blood pressure measurements. (d) Diastolic blood pressure measurement error curve. (e) Heartbeat measurement. (f) Heartbeat measurement error curve.

consuming. This study proposed the use of cloud technology and IPSO to solve these problems. After searches of serious conditions in the top 10% of the staff in the huge database, this study used Initiative to inform related medical staff for further diagnosis and early treatment. This paper identified the most serious cases from 120 records data and then compiled the data in Excel (Fig. 25).

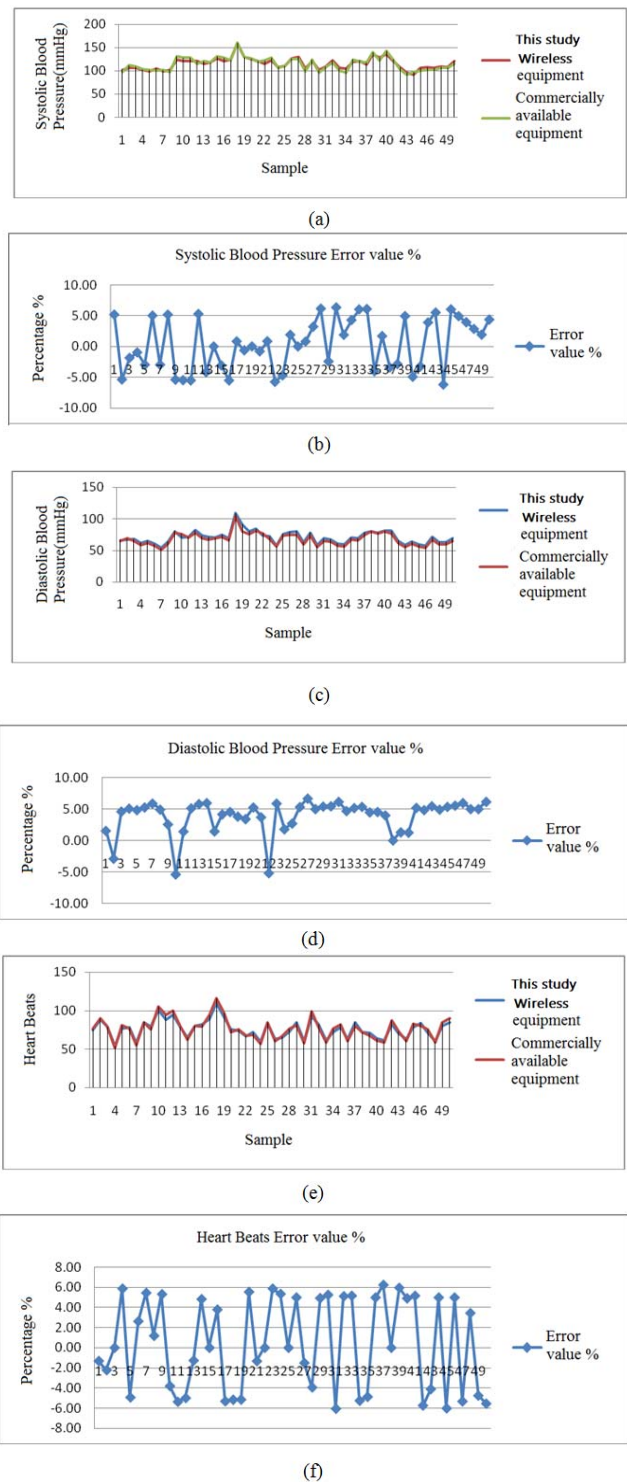


Fig. 24. Comparison of proposed measurement with existing wireless instrument measurement in terms of error ratio value. (Wireless transmission environment-based) (a) Systolic blood pressure measurements. (b) Systolic blood pressure measurement error curve. (c) Diastolic blood pressure measurements. (d) Diastolic blood pressure measurement error curve. (e) Heartbeat measurement. (f) Heartbeat measurement error curve.

This study weighted various physiological data as suggested by the Taiwan Department of Health, including blood pressure, blood oxygen, BMI, heart rate standard to determine the classification table, with reference to our previous study [36], [37].

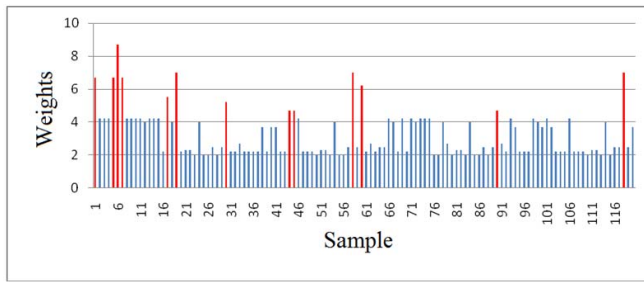


Fig. 25. IPSO Weight simulation results.

When the physiological data are within the normal range, the weight value is set to 0.5. The physiological data are weighted according to severity, *i.e.*, a value in a higher than normal range has a high weigh value. For example: if the oxygen concentration is less than 94% to 92%, the weight value is set to 3. Since the literature [28] indicates that low oxygen can cause a mortality rate up to 45.5%, the oxygen concentration is weighted more heavily than other physiological data. Other physiological data are based on our previous research results of the reference standard to constant weight.

This study proposed IPSO to the global random optimization search by using the Matlab simulation results. Based on the hazardous areas of standard data, the measured data for each subject were weighted, and the IPSO simulation program was used to identify the top 10% of the most serious of the information. Matlab simulation program showed the most serious cases identified based on the huge amount of data. The business community can use the proposed system to inform staff priority to a related medical staff first and to avoid delays in treatment caused by the incidence of death [38], [39].

## VIII. CONCLUSION AND FUTURE STUDIES

In recent years, medical resources have been reduced by changes in social development patterns, including (1) an aging social structure, *i.e.*, the increasing proportion of the elderly population with chronic diseases and (2) government policies making science and technology industries the center of economic growth and resulting in work stress and fatigue phenomena. Therefore, this study designed a cloud-based mobile physiological measurement system with analysis functions for personal remote health care system.

In recent years, the Taiwan population has shown an aging trend. Thus, elderly care is gradually being recognized as an important issue. According to 2012 statistics, an average of 2.87 youths now supports one elderly person and one juvenile person. By 2060, an average of one young person will be required to support one elderly person and one juvenile person. Hence, this study is aimed at integrating non-invasive physiological testing equipment with home care for the elderly, including ECG measurement, blood pressure measurement, and blood oxygen measurement. The proposed physiological integration platform combines the currently popular Android system with IOT and a cloud system.

The physiological measurement integration system platform is installed with an LCD display, which is mainly used to

display the physiological data measured by the physiological capture equipment. The transmission devices (Bluetooth, ZigBee) of the physiological measurement integration platform are then used to send physiological signals to a mobile handheld device (e.g., PC, smart phone), which enables remote monitoring by a network and the use of a medical cloud system to store the personal medical data of the subject in order to facilitate disease diagnosis and save medical resources from unnecessary waste. The proposed method has the following four advantages: (1) medical equipment resource integration and sharing; medical equipment are integrated so that they can share the platform; (2) the use of a cloud server to record the complete personal data of the subjects and to judge the physiological conditions of the subject in real time; (3) remote care to monitor the physiological data of the subject through a mobile phone platform so that the subject can be monitored in real time; and (4) IPSO analysis to determine the optimal physiological data through PSO and to set danger levels according to the methods of this study so that the system can be used to identify risk groups for sudden death and that can potentially result from cardiovascular diseases.

## REFERENCES

- [1] C. Ramon, A. Clarion, C. Gehin, C. Petit, C. Collet, and A. Dittmar, "An integrated platform to assess driver's physiological and functional states," in *Proc. 30th Annu. Int. Conf. IEEE EMBC*, Aug. 2008, pp. 506–509.
- [2] H.-Y. Chen, J.-R. Wang, K.-Y. Lu, and K.-L. Wen, "The evaluation of liver function via grey relational analysis," in *Proc. IEEE Int. Conf. SMC*, Oct. 2009, pp. 767–770.
- [3] F. M. Matsubara, S. Miura, S. Imai, and S. Akatsu, "DTV architecture design for multimedia network environments," *IEEE Trans. Consum. Electron.*, vol. 51, no. 1, pp. 324–328, Feb. 2005.
- [4] J. W. Kwak and C. S. Jhon, "High-performance embedded branch predictor by combining branch direction history and global branch history," *IET Comput. Digit. Tech.*, vol. 2, no. 2, pp. 142–154, Mar. 2008.
- [5] M. R. Neuman, G. D. Baura, S. Meldrum, O. Soykan, M. E. Valentinuzzi, R. S. Leder, S. Micera, and Y.-T. Zhang, "Advances in medical devices and medical electronics," *Proc. IEEE*, vol. 100, no. 13, pp. 1537–1550, May 2012.
- [6] H. M. La, R. S. Lim, J. Du, S. Zhang, G. Yan, and W. Sheng, "Development of a small-scale research platform for intelligent transportation systems," *IEEE Trans. Intell. Transp. Syst.*, vol. 13, no. 4, pp. 1753–1762, Dec. 2012.
- [7] J. M. L. P. Caldeira, J. J. P. C. Rodrigues, and P. Lorenz, "Toward ubiquitous mobility solutions for body sensor networks on healthcare," *IEEE Commun. Mag.*, vol. 50, no. 5, pp. 108–115, May 2012.
- [8] F. Hu, Q. Hao, M. Lukowiak, Q. Sun, K. Wilhelm, S. Radziszowski, and Y. Wu, "Trustworthy data collection from implantable medical devices via high-speed security implementation based on IEEE 1363," *IEEE Trans. Inf. Technol. Biomed.*, vol. 14, no. 6, pp. 1397–1404, Nov. 2010.
- [9] R. S. H. Istepanian and Y.-T. Zhang, "Guest editorial introduction to the special section: 4G health—The long-term evolution of m-health," *IEEE Trans. Inf. Technol. Biomed.*, vol. 16, no. 1, pp. 1–5, Jan. 2012.
- [10] D. Lu and T. Liu, "The application of IOT in medical system," in *Proc. ITME*, vol. 1, pp. 272–275, Dec. 2011.
- [11] H. J. La and S. D. Kim, "A service-based approach to developing android mobile internet device (MID) applications," in *Proc. IEEE Int. Conf. SOCA*, Aug. 2009, pp. 1–7.
- [12] W. Zhaohui, R. Murmura, and A. Stavrou, "Implementing and optimizing an encryption filesystem on android," in *Proc. IEEE 13th Int. Conf. MDM*, Nov. 2012, pp. 52–62.
- [13] W.-N. Chen, J. Zhang, Y. Lin, N. Chen, Z.-H. Zhan, H. S.-H. Chung, Y. Li, and Y.-H. Shi, "Particle swarm optimization with an aging leader and challengers," *IEEE Trans. Evol. Comput.*, vol. 17, no. 2, pp. 241–258, Apr. 2013.

- [14] W. Zhitian, W. Yuanxin, H. Xiaoping, and W. Meiping, "Calibration of three-axis magnetometer using stretching particle swarm optimization algorithm," *IEEE Trans. Instrum. Meas.*, vol. 62, no. 2, pp. 281–292, Feb. 2013.
- [15] R. S. Dilmaghani, H. Bobarshad, M. Ghavami, S. Choobkar, and C. Wolfe, "Wireless sensor networks for monitoring physiological signals of multiple patients," *IEEE Trans. Biomed. Circuits Syst.*, vol. 5, no. 4, pp. 347–356, Aug. 2011.
- [16] R.-G. Lee, K.-C. Chen, C.-C. Hsiao, and C.-L. Tseng, "A mobile care system with alert mechanism," *IEEE Trans. Inf. Technol. Biomed.*, vol. 11, no. 5, pp. 507–517, Sep. 2007.
- [17] R. Jafari, H. Noshadi, S. Ghiasi, and M. Sarrafzadeh, "Adaptive electrocardiogram feature extraction on distributed embedded systems," *IEEE Trans. Parallel Distrib. Syst.*, vol. 17, no. 8, pp. 797–807, Aug. 2006.
- [18] E. Kafeza, D. K. W. Chiu, S. C. Cheung, and M. Kafeza, "Alerts in mobile healthcare applications: Requirements and pilot study," *IEEE Trans. Inf. Technol. Biomed.*, vol. 8, no. 2, pp. 173–181, Jun. 2004.
- [19] S. Tayyaba, M. W. Ashraf, and N. Afzulpurkar, "Simulation and fabrication of blood filtration system for patients with kidney diseases," *IET Commun.*, vol. 6, no. 18, pp. 3213–3221, Dec. 2012.
- [20] L. Lam, J. Bilek, and J. Atkinson, "Studies on the temperature distribution of a thick film transcutaneous oxygen sensor and its thermal influences on oxygen measurement," *IEEE Trans. Biomed. Eng.*, vol. 53, no. 11, pp. 2341–2346, Nov. 2006.
- [21] S. Farshchi, A. Pesterev, P. H. Nuyujukian, I. Mody, and J. W. Judy, "Bi-Fi: An embedded sensor/system architecture for remote biological monitoring," *IEEE Trans. Inf. Technol. Biomed.*, vol. 11, no. 6, pp. 611–618, Nov. 2007.
- [22] C. Wang, Q. Xiaojun, L. Yanfei, and Y. Chengbo, "Low power research and design in plant eco-physiological monitoring system based on ZigBee," in *Proc. WAC*, Sep. 2010, pp. 67–71.
- [23] L. Xiaomei, Z. Zhentao, and Y. Jing, "Wearable monitoring system with physiological parameter based on ZigBee," in *Proc. Int. Conf. CMCE*, Jul. 2010, pp. 329–332.
- [24] C.-T. Lin, Y.-C. Chen, T.-Y. Huang, T.-T. Chiu, L.-W. Ko, S.-F. Liang, H.-Y. Hsieh, S.-H. Hsu, and J.-R. Duann, "Development of wireless brain computer interface with embedded multitask scheduling and its application on real-time driver's drowsiness detection and warning," *IEEE Trans. Biomed. Eng.*, vol. 55, no. 5, pp. 1582–1591, May 2008.
- [25] J. H. Shorter, D. D. Nelson, J. B. McManus, M. S. Zahniser, and D. K. Milton, "Multicomponent breath analysis with infrared absorption using room-temperature quantum cascade lasers," *IEEE Sensors J.*, vol. 10, no. 1, pp. 76–84, Jan. 2010.
- [26] M. A. M. de Oca, T. Stutzle, K. Van den Enden, and M. Dorigo, "Incremental social learning in particle swarms," *IEEE Trans. Syst., Man, Cybern., B, Cybern.*, vol. 41, no. 2, pp. 368–384, Apr. 2011.
- [27] T. Niknam, M. R. Narimani, J. Aghaei, and R. Azizpanah-Abarghoee, "Improved particle swarm optimisation for multi-objective optimal power flow considering the cost, loss, emission and voltage stability index," *IET Generat., Transmiss. Distrib.*, vol. 6, no. 6, pp. 515–527, Jun. 2012.
- [28] W.-T. Sung and Y.-C. Chiang, "Improved particle swarm optimization algorithm for android medical care IOT using modified parameters," *J. Med. Syst.*, vol. 36, no. 6, pp. 3755–3763, Dec. 2012.
- [29] W.-T. Sung and M.-H. Tsai, "Data fusion of multi-sensor for IOT precise measurement based on improved PSO algorithms," *Comput. Math. Appl.*, vol. 64, no. 5, pp. 1450–1461, Sep. 2012.
- [30] W.-T. Sung and M.-H. Tsai, "Multi-sensor wireless signal aggregation for environmental monitoring system via multi-bit data fusion," *Appl. Math. Inf. Sci.*, vol. 5, no. 3, pp. 589–603, 2011.
- [31] W.-T. Sung, J.-H. Chen, M.-H. Wang, and Y.-C. Hsu, "Remote medical care system design based on RFID and ZigBee technology via wireless sensors network," *Int. J. Innovative Comput., Inf. Control*, vol. 6, no. 11, pp. 5203–5220, Nov. 2010.
- [32] C. De Capua, A. Meduri, and R. Morello, "A smart ECG measurement system based on web-service-oriented architecture for telemedicine applications," *IEEE Trans. Instrum. Meas.*, vol. 59, no. 10, pp. 2530–2538, Oct. 2010.
- [33] A. Burgos, A. Goñi, A. Illarramendi, and J. Bermudez, "Real-time detection of apneas on a PDA," *IEEE Trans. Inf. Technol. Biomed.*, vol. 14, no. 4, pp. 995–1002, Jul. 2010.
- [34] P. Arpaia, C. Manna, G. Montenero, and G. D'Addio, "In-time prognosis based on swarm intelligence for home-care monitoring: A case study on pulmonary disease," *IEEE Sensors J.*, vol. 12, no. 3, pp. 692–698, Mar. 2012.
- [35] B.-J. Park, E.-H. Jang, S.-H. Kim, C. Huh, and J.-H. Sohn, "Seven emotion recognition by means of particle swarm optimization on physiological signals: Seven emotion recognition," in *Proc. 9th IEEE ICNSC*, Apr. 2012, pp. 277–282.
- [36] W.-T. Sung, J.-H. Chen, and K.-W. Chang, "Study on a real-time BEAM system for diagnosis assistance based on system on chips," *Sensors*, vol. 13, no. 5, pp. 6552–6577, May 2013.
- [37] W.-T. Sung, J.-H. Chen, and K.-J. Chang, "ZigBee based multi-purpose electronic score design and implementation using EOG," *Sens. Actuators A, Phys.*, vol. 190, no. 1, pp. 141–152, 2013.
- [38] L. Xuanya, C. Linlin, Y. Minghua, W. Hongyu, T. Chengping, and C. Bin, "Multi-decision making based PSO optimization in airborne mobile sensor network deployment," in *Proc. IEEE 6th Int. Symp. Embedded MCSoc*, Sep. 2012, pp. 128–134.
- [39] C. Scully, L. Jinseok, J. Meyer, A. M. Gorbach, D. Granquist-Fraser, Y. Mendelson, and K. H. Chon, "Physiological parameter monitoring from optical recordings with a mobile phone," *IEEE Trans. Biomed. Eng.*, vol. 59, no. 2, pp. 303–306, Feb. 2012.



**Wen-Tsai Sung** is with the Department of Electrical Engineering, National Chin-Yi University of Technology, Taichung, Taiwan, as an Associate Professor, and a Vice-Dean of Academic Affairs. He received the Ph.D. and M.S. degrees from the Department of Electrical Engineering, National Central University, Taoyuan, Taiwan, in 2007 and 2000, respectively. He has received the 2009 JMBE Best Annual Excellent Paper Award and the Dragon Thesis Award sponsored by the Acer Foundation. His research interests include wireless sensors network, data fusion, system biology, system on chip, computer-aided design for learning, bioinformatics, and biomedical engineering. He has published a number of international journal and conference articles. Currently, he is the Chief of Wireless Sensors Networks Laboratory. He serves as the Editor-in-Chief of two international journals, *Communications in Information Science and Management Engineering (CISME)* and *Journal of Vibration Analysis, Measurement, and Control (JVAMC)*. He also serves as Associate Editor and Guest Editor of the SCI journal *IET Systems Biology*.



**Jui-Ho Chen** is with the Department of Electrical Engineering, National Chin-Yi University of Technology, Taichung, Taiwan, as an Associate Professor. His research interests include wireless sensors network, data fusion, and biomedical engineering. He has published a number of international journal and conference articles.



**Kung-Wei Chang** is currently pursuing the master's degree at the Department of Electrical Engineering, National Chin-Yi University of Technology, Taichung, Taiwan. His current research activities include the wireless sensors networks, SoC system, and data fusion. Currently, he is a member of Wireless Sensors Networks Laboratory.